

# Evidence of X-ray Synchrotron Emission from Electrons Accelerated to 40 TeV in the Supernova Remnant Cassiopeia A

G. E. Allen<sup>1</sup>, J. W. Keohane<sup>2</sup>, E. V. Gotthelf<sup>3</sup>, R. Petre, and K. Jahoda  
NASA Goddard Space Flight Center, Laboratory for High Energy Astrophysics, Code 662,  
Greenbelt, MD 20771

R. E. Rothschild, R. E. Lingenfelter, W. A. Heindl, D. Marsden, D. E. Gruber, M. R. Pelling, and P. R. Blanco  
University of California, San Diego, Center for Astrophysics & Space Sciences, Code 0111,  
9500 Gilman Drive, La Jolla, CA 92093

## ABSTRACT

We present the 2–60 keV spectrum of the supernova remnant Cassiopeia A measured using the Proportional Counter Array and the High Energy X-ray Timing Experiment on the Rossi X-ray Timing Explorer satellite. In addition to the previously reported strong emission-line features produced by thermal plasmas, the broad-band spectrum has a high-energy “tail” that extends to energies at least as high as 120 keV. This tail may be described by a broken power law that has photon indices of  $\Gamma_1 = 1.8_{-0.6}^{+0.5}$  and  $\Gamma_2 = 3.04_{-0.13}^{+0.15}$  and a break energy of  $E_b = 15.9_{-0.4}^{+0.3}$  keV. We argue that the high-energy component, which dominates the spectrum above about 10 keV, is produced by synchrotron radiation from electrons that have energies up to at least 40 TeV. This conclusion supports the hypothesis that Galactic cosmic rays are accelerated predominantly in supernova remnants.

*Subject headings:* ISM: individual (Cassiopeia A) — supernova remnants — radiation mechanisms: non-thermal — acceleration of particles — cosmic rays — X-rays: general

---

<sup>1</sup> NRC-NASA GSFC Postdoctoral Research Associate; glenn.allen@gsfc.nasa.gov

<sup>2</sup>University of Minnesota, Astronomy Department

<sup>3</sup>Universities Space Research Association

## 1. Introduction

Galactic cosmic rays that have energies below  $\sim 10^{14}$  eV are believed to be accelerated predominantly in the shocks of supernova remnants (SNRs). Prior to the last two years, little experimental evidence existed to support this hypothesis. Radio measurements show that many SNRs emit synchrotron radiation from nonthermal electrons, but these measurements are not sensitive to emission from electrons that have energies greater than  $\sim 10^{10}$  eV. Gamma-ray measurements at energies  $< 10^{10}$  eV also show that some SNRs contain nonthermal particles (Esposito et al. 1996), but the interpretation of these results is controversial (Allen et al. 1995; Lessard et al. 1995; de Jager & Mastichiadis 1997; Gaisser, Protheroe, & Stanev 1997; Sturmer et al. 1997). However, recent measurements of X-ray spectra of SNRs have provided the best evidence to date that SNRs may be responsible for most of the cosmic-ray acceleration in the Galaxy.

While the X-ray spectra of SNRs have traditionally been modeled as thermal emission from shock-heated plasmas, the spectra of SN 1006 (Koyama et al. 1995) and RX J1713.7–3946 (Koyama et al. 1997) are dominated by nonthermal emission interpreted to be synchrotron radiation from electrons having energies up to  $\sim 10^{14}$  eV. IC 443 may also contain a site that emits X-ray synchrotron radiation from electrons having energies at least as high as  $2 \times 10^{13}$  eV (Keohane et al. 1997).

We present the 2–60 keV spectrum of Cassiopeia A (Cas A) measured using detectors on the Rossi X-ray Timing Explorer (RXTE) satellite. This spectrum has a high-energy “tail” that extends to energies at least as high as 60 keV. The strong emission lines in the 0.5–10 keV spectrum (Holt et al. 1994; Jansen et al. 1988; Tsunemi et al. 1986) can be described by two-temperature thermal plasma models whose flux is dominated by emission from either swept-up material (Borkowski et al. 1996) or shocked ejecta (Vink, Kaastra, & Bleeker 1996; Jansen et al. 1988). However, these models do not describe the higher-energy tail of the spectrum (Favata et al. 1997; Pravdo & Smith 1979; Hatsukade & Tsunemi 1992) that has been detected up to at least 120 keV (The et al. 1996). The results of our analysis imply that both the X-ray tail and the radio spectrum ( $S_\nu = 2723(\nu/1 \text{ GHz})^{-0.77}$  Jy, Baars et al. 1977) are produced by synchrotron radiation from a common population of nonthermal electrons whose spectrum extends up to at least  $4 \times 10^{13}$  eV.

## 2. Data and Analysis

Between 1996 March 31 and 1996 April 17, Cas A was observed for 186 ks using the Proportional Counter Array (PCA) and the High Energy X-ray Timing Experiment

(HEXTE) on the RXTE satellite. The PCA (Jahoda et al. 1996) and HEXTE (Gruber et al. 1996) comprise a 2-250 keV spectrophotometer that has an energy resolution  $\sim 10\text{--}30\%$  and a collecting area of about  $7000\text{ cm}^2$  at 6 keV and of  $800\text{ cm}^2$  at 60 keV.

Figures 1 and 2 show the PCA and HEXTE spectra of Cas A for 91 ks of the PCA data and for 96 ks of HEXTE data. Because the strong emission lines may be fit by models with two thermal plasmas and with fluorescent  $K\alpha$  emission from iron in dust grains (Borkowski & Szymkowiak 1997), we model these features using two Raymond-Smith components and a 6.40 keV Gaussian. While such a model provides an adequate fit to the 0.5–10 keV spectrum, it does not fit the spectrum above  $\sim 10$  keV (fig. 2). At least one more component is needed to model the broad-band X-ray spectrum.

We fit the broad-band spectrum using models that include only one additional component that is either a thermal bremsstrahlung, a power law, a power law that has an exponential cutoff, or a broken power law. In general, the high-energy spectrum is better fit by the nonthermal components than a thermal bremsstrahlung component. Furthermore, the spectrum is better fit by a broken power law than a power law or a cut off power law. Table 1 summarizes the best fit models that include either a broken power law component or a thermal bremsstrahlung component. Abundances of some line-emitting elements are listed in the table because the abundances depend on the high-energy component. The abundances should be regarded as rough estimates because a better treatment requires plasmas that are not in ionization equilibrium. The values of  $\chi^2$  in table 1 were computed for only the  $\geq 10$  keV portion of the PCA and HEXTE spectra where the high-energy component dominates the flux. The “ $1\sigma$ ” errors quoted in this paper, which may be underestimated, were computed by finding the extrema of the  $\chi^2$  contour that has a value of  $\chi^2$  which is larger than the minimum value by 2.3.

Figure 1 shows the spectrum of the best fit model “folded” through the PCA and HEXTE response matrices. The lower panel of this figure shows the ratio of the measured spectra to this model. Aside from the uncertainty in the cross calibration of the PCA and HEXTE, this ratio is dominated by systematic errors in the response matrix and the background spectrum for the PCA and by statistical errors for the HEXTE. For example, the features near 2 keV and between 5 and 8 keV in the lower panel of figure 1 reflect inaccuracies of the v2.0.2 PCA response matrix that are observed when modeling PCA spectra for other sources, such as the Crab (Jahoda et al. 1996). These features are not evident in the fit to the spectrum of the Gas Imaging Spectrometer no. 2 (GIS2) on the Advanced Satellite for Cosmology and Astrophysics.

Figure 2 shows the GIS2, PCA, HEXTE, and OSSE (Oriented Scintillation Spectrometer Experiment on the Compton Gamma Ray Observatory satellite, The et al.

1996) spectral data and the “unfolded” spectrum of the best fit model (solid curve). For comparison, figure 2 also shows the spectrum of a model that includes only the two Raymond-Smith components and the Fe K $\alpha$  dust component (dashed curve).

### 3. Discussion

The spectra of several emission mechanisms—thermal and nonthermal bremsstrahlung, a pulsar, inverse Compton scattering, and synchrotron radiation—could be described by a broken power law in the range of 10–63 keV. Each possibility is discussed in the context of Cas A.

It is unlikely that the high-energy X-ray tail of Cas A is thermal. As shown in figure 2 and table 1, the broad-band X-ray spectrum is not well fit by two or three thermal component models. Furthermore, a physical interpretation of a model that has three thermal components is difficult. Two of the components could be associated with the forward-shocked circumstellar material and the reverse-shocked ejecta. The third might result from a nonuniform distribution of the circumstellar or ejected matter. However, spatially-resolved spectroscopy shows that Cas A has similar plasma conditions across the remnant (Holt et al. 1994).

Asvarov et al. (1989) suggest that the high-energy X-ray spectrum of Cas A is dominated by nonthermal bremsstrahlung emission. However, an estimate of the nonthermal bremsstrahlung spectrum (fig. 3) yields a 20–50 keV effective photon index of  $\sim 1.9$ , which is significantly smaller than the fitted index of  $3.04_{-0.13}^{+0.15}$ . Therefore, the X-ray tail of Cas A appears to be too steep to be consistent with a nonthermal bremsstrahlung emission process.

Although pulsars can produce nonthermal X-ray continua, it is unlikely that the high-energy tail of Cas A is produced by a pulsar. Analyses of X-ray (Allen et al. 1997; Pravdo & Smith 1979), radio (Woan & Duffett-Smith 1993) and optical (Horowitz, Papaliolios, & Carleton 1971) data reveal no evidence of pulsation and no bright point-like feature is observed near the center of the remnant (Fabian et al. 1980; Holt et al. 1994; Jansen et al. 1988).

An inverse Compton spectrum could be consistent with the shape of the tail, but the estimated flux is a factor of  $\sim 10^4$  smaller than the measured flux at energies in the range of 10–63 keV (fig. 3).

In contrast to the other emission processes, both the shape and the flux of the

high-energy component of the X-ray spectrum of Cas A are consistent with a synchrotron radiation mechanism. In general, the synchrotron spectrum of a SNR is expected to span the entire range from radio to X-ray energies and to steepen gradually at or near X-ray energies (Reynolds 1997). This expectation is consistent with the multiwavelength spectrum of Cas A because the extrapolation of the radio synchrotron spectrum to X-ray energies does not lie above the observed thermal emission at infrared wavelengths or below the X-ray spectrum (fig. 3) and because the broken power law of table 1 approximately describes a gradually steepening spectrum. The synchrotron spectrum of figure 3 is a power-law spectrum with a  $e^{-\sqrt{E_\gamma/1 \text{ keV}}}$  cutoff. This photon spectrum corresponds to a power-law electron spectrum with a  $e^{-(E_e/8 \times 10^{12} \text{ eV})}$  cutoff and assumes that the spectral distribution of synchrotron photons emitted by electrons of a common energy is a delta function. A better estimate of the synchrotron spectrum, which is expected to steepen more gradually than  $e^{-\sqrt{E_\gamma/1 \text{ keV}}}$  (Reynolds 1997), requires a numerical simulation of the particle acceleration conditions appropriate for Cas A including the effects (1) of synchrotron losses on the electron spectrum, (2) of possible curvature in the electron spectrum (Mezger et al. 1986; Ellison & Reynolds 1991), and (3) of the spectral distribution of synchrotron photons for electrons of a given energy.

Figure 3 shows the radio (Baars et al. 1977), infrared (Mezger et al. 1986), RXTE, OSSE (The et al. 1996), EGRET (Esposito et al. 1996), and Whipple (Lessard et al. 1995) spectral data of Cas A. The estimated synchrotron spectrum is a single power law that has a  $e^{-\sqrt{E_\gamma/1 \text{ keV}}}$  cutoff. Also shown are estimates of the photon spectra produced by nonthermal bremsstrahlung, by inverse Compton scattering of the cosmic microwave background radiation, and by the decay of neutral pions. These latter three estimates were computed for electron and proton spectra that have a common spectral index of 2.54 using equation 13 and figure 3 of Gaisser et al. (1997). The electron density spectrum is assumed to be  $7 \times 10^{-8} \text{ cm}^{-3} \text{ GeV}^{-1}$  at 1 GeV. The density of accelerated nuclei is assumed to be one hundred times larger than the density of accelerated electrons independent of energy. The nonthermal bremsstrahlung and  $\pi^0$  decay spectra were computed for a density of nuclei in Cas A of  $30 \text{ cm}^{-3}$ . The shape of the nonthermal bremsstrahlung spectrum at energies below 1 MeV is based on the shape of the nonthermal bremsstrahlung spectrum of Sturmer et al. (1997, fig. 11).

#### 4. Conclusion

The RXTE data reveal that the X-ray continuum of Cas A has a nonthermal high-energy “tail.” The tail (1) is qualitatively consistent with a simple model of synchrotron emission

from SNRs, (2) is inconsistent with the expected shape of a nonthermal bremsstrahlung spectrum, and (3) is inconsistent with the estimated inverse Compton flux. No evidence of pulsation or of a bright central point-like feature has been reported. Therefore, the tail is most likely produced by synchrotron radiation.

X-ray synchrotron emission has important implications for particle acceleration in Cas A. The energy of a synchrotron photon,  $E_\gamma$ , is related to the energy of the emitting electron and the magnetic field strength by  $E_\gamma \sim 0.6 B_{\mu\text{G}} E_{14}^2$  keV, where  $B_{\mu\text{G}}$  is the magnetic field strength in units of  $\mu\text{G}$  and  $E_{14}$  is the energy of the electron in units of  $10^{14}$  eV. If the synchrotron spectrum extends to energies at least as high as 120 keV and the magnetic field is 1 mG (the “equipartition” value, e.g. Longair 1994), the accelerated electron spectrum extends up to at least  $4 \times 10^{13}$  eV. Since electrons and protons are expected to be accelerated in the same manner at energies much larger than the rest mass energy of the proton (Ellison & Reynolds 1991), this result provides strong evidence for the acceleration of cosmic-ray protons in Cas A to the same energies. The calculation of the equipartition value of the magnetic field leads to an estimate of the total amount of energy in accelerated protons and electrons of  $\sim 3 \times 10^{49}$  erg (Longair 1994). This amount of energy is comparable to the average amount of energy required from a Galactic SNR ( $\sim 3\text{--}10 \times 10^{49}$  erg), over the lifetime of the remnant, if all of the Galactic cosmic rays are accelerated in SNRs.

Cas A is the fourth SNR reported to exhibit evidence of X-ray synchrotron radiation. Collectively, the results for Cas A, SN 1006 (Koyama et al. 1995), RX J1713.7–3946 (Koyama et al. 1997), and IC 443 (Keohane et al. 1997) support the hypothesis that Galactic cosmic rays are accelerated predominantly in SNRs.

We thank Apostolos Mastichiadis and Steve Reynolds for advice about the expected shape of the spectrum of synchrotron radiation. We are grateful to Jacco Vink for many stimulating and thoughtful discussions about the data and about the implications of the data. We appreciate Jennifer Allen’s careful review of the manuscript. This work was performed while GEA held a NRC-NASA GSFC Research Associateship. The work at UCSD was supported by NASA contract NAS5-30720 and NASA grant NAG5-3375.

## REFERENCES

- Allen, G. E., et al. 1995, *ApJ*, 448, L25
- Allen, G. E., et al. 1997, in preparation
- Asvarov, A. I., Guseinov, O. Kh., Dogel, V. A., & Kasumov, F. K. 1989, *Sov. Astron.*, 33, 532
- Baars, J. W. M., Genzel, R., Pauliny-Toth, I. I. K., & Witzel, A. 1977, *A&A*, 61, 99
- Borkowski, K. J., & Szymkowiak, A. E. 1997, *ApJ*, submitted
- Borkowski, K. J., Szymkowiak, A. E., Blondin, J. M., & Sarazin, C. L. 1996, *ApJ*, 466, 866
- de Jager, O. C., & Mastichiadis, A. 1997, *ApJ*, submitted
- Ellison, D. C., & Reynolds, S. P. 1991, *ApJ*, 382, 242
- Esposito, J. A., Hunter, S. D., Kanbach, G., & Sreekumar, P. 1996, *ApJ*, 461, 820
- Fabian, A. C., Willingale, R., Pye, J. P., Murray, S. S., & Fabbiano, G. 1980, *MNRAS*, 193, 175
- Favata, F., et al. 1997, in preparation
- Gaisser, T. K., Protheroe, R. J., & Stanev, T. 1997, *ApJ*, submitted
- Ginzburg, V. L., & Syrovatskii, S. I. 1964, *The Origin of Cosmic Rays* (New York: Macmillan)
- Gruber, D. E., Blanco, P. R., Heindl, W. A., Pelling, M. R., Rothschild, R. E., & Hink, P. L. 1996, *BAAS*, 120, 641
- Hatsukade, I., & Tsunemi, H. 1992, in *Frontiers of X-Ray Astronomy*, ed. Y. Tanaka & K. Koyama (Tokyo: Universal Academy Press, Inc.), 387
- Holt, S. S., Gotthelf, E. V., Tsunemi, H., & Negoro, H. 1994, *PASJ*, 46, L151
- Horowitz, P., Papaliolios, C., & Carleton, N. P. 1971, *ApJ*, 163, L5
- Jahoda, K., Swank, J. H., Giles, A. B., Stark, M. J., Strohmayer, T., Zhang, W., & Morgan, E. H. 1996, in *EUV, X-ray and Gamma-ray Instrumentation for Space Astronomy VII*, ed. Siegmund, O. H. W., & Grummin, M. A. *Proc. SPIE*, 2808, 59

- Jansen, F., Smith, A., Bleeker, J. A. M., de Korte, P. A. J., Peacock, A., & White, N. E. 1988, *ApJ*, 331, 949
- Keohane, J. W., Petre, R., Gotthelf, E. V., Ozaki, M., & Koyama, K. 1997, *ApJ*, in press
- Koyama, K., Kinugasa, K., Matsuzaki, K., Nishiuchi, M., Sugizaki, M., Torii, K., Yamauchi, S., & Aschenbach, B. 1997, *PASJ*, 49, in press
- Koyama, K., Petre, R., Gotthelf, E. V., Hwang, U., Matsuura, M., Ozaki, M., & Holt, S. S. 1995, *Nature*, 378, 255
- Lessard, R. W., et al. 1995, in *Proceedings of the 24th International Cosmic Ray Conference*, 2, 475
- Longair, M. S. 1994, *High Energy Astrophysics*, Vol. 2 (Cambridge: Cambridge University Press), sec. 19.5
- Mezger, P. G., Tuffs, R. J., Chini, R., Kreysa, E., Gemünd, H.-P. 1986, *A&A*, 167, 145
- Pravdo, S. H., & Smith, B. W. 1979, *ApJ*, 234, L195
- Reynolds, S. P. 1997, *ApJ*, submitted
- Sturmer, S. J., Skibo, J. G., Dermer, C. D., & Mattox, J. R. 1997, *ApJ*, submitted
- The, L.-S., Leising, M. D., Kurfess, J. D., Johnson, W. N., Hartmann, D. H., Gehrels, N., Grove, J. E., & Purcell, W. R. 1996, *A&AS*, 120, 357
- Tsunemi, H., Yamashita, K., Masai, K., Hayakawa, S., & Koyama, K. 1986, *ApJ*, 306, 248
- Vink, J., Kaastra, J. S., & Bleeker, J. A. M. 1996, *A&A*, 307, L41
- Woan, G., & Duffett-Smith, P. J. 1993, *MNRAS*, 260, 693



Fig. 1.— The PCA and HEXTE count spectra of Cas A. The histogram is the broken power-law model of table 1. The lower panel shows the ratio of the data to the histogram. See text for details.

Fig. 2.— The GIS2, PCA, HEXTE, and OSSE (The et al. 1996) photon spectra of Cas A. The solid curve shows the broken power-law model of table 1. The dashed curve shows what the shape of the spectrum is if no high-energy component is included in the fit.

Fig. 3.— The multiwavelength photon spectrum of Cas A. The four broken curves are estimates of the fluxes from synchrotron radiation (S), from nonthermal bremsstrahlung (NB), from inverse Compton scattering of the cosmic microwave background (IC), and from the decay of neutral pions ( $\pi^0$ ). See text for details.

Table 1. Parameters of the Spectral Models<sup>a</sup>

Broken Power Law									
$\Gamma_1$ ( $E < E_b$ )	$E_b$ (keV)	$\Gamma_2$ ( $E > E_b$ )	Flux at 1 keV (ph cm <sup>-2</sup> s <sup>-1</sup> keV <sup>-1</sup> )	Abundance <sup>b</sup>					$\chi^2$ <sup>c</sup> (69 dof)
				Si	S	Ar	Ca	Fe	
				(Solar)					
1.8 <sup>+0.5</sup> <sub>-0.6</sub>	15.9 <sup>+0.3</sup> <sub>-0.4</sub>	3.04 <sup>+0.15</sup> <sub>-0.13</sub>	0.038	2.1	4.3	8.3	2.6	0.6	105
Thermal Bremsstrahlung									
$kT$ (keV)	$\int n_e n_i dV$ <sup>d</sup> (10 <sup>58</sup> cm <sup>-3</sup> )	Abundance <sup>b</sup>					$\chi^2$ <sup>c</sup> (71 dof)		
		(as above)							
23.7 <sup>+0.8</sup> <sub>-0.7</sub>	1.16 ± 0.04	2.0	4.1	7.7	2.3	0.6	236		

<sup>a</sup>These fits also include two Raymond-Smith components that have temperatures of  $kT_1 = 0.6$  keV and  $kT_2 = 2.9$  keV and a 6.40 keV Gaussian component ( $1.3 \times 10^{-3}$  photons cm<sup>-2</sup> s<sup>-1</sup>) for  $K\alpha$  emission from iron in dust grains. The fit column density  $n_H = 1.1 \times 10^{22}$  H atoms cm<sup>-2</sup>.

<sup>b</sup>The Si, S, and Ar abundances pertain to the  $kT_1 = 0.6$  keV plasma. The Ca and Fe abundances pertain to the  $kT_2 = 2.9$  keV plasma.

<sup>c</sup>For the energy range from 10 to 63 keV.

<sup>d</sup>The quantities  $n_e$  and  $n_i$  are the electron and ion densities respectively. The average value of  $n_e n_i$  is  $\sim 25$  cm<sup>-6</sup> for a distance of 3.4 kpc and a filling fraction of 1/4.

Figure 1

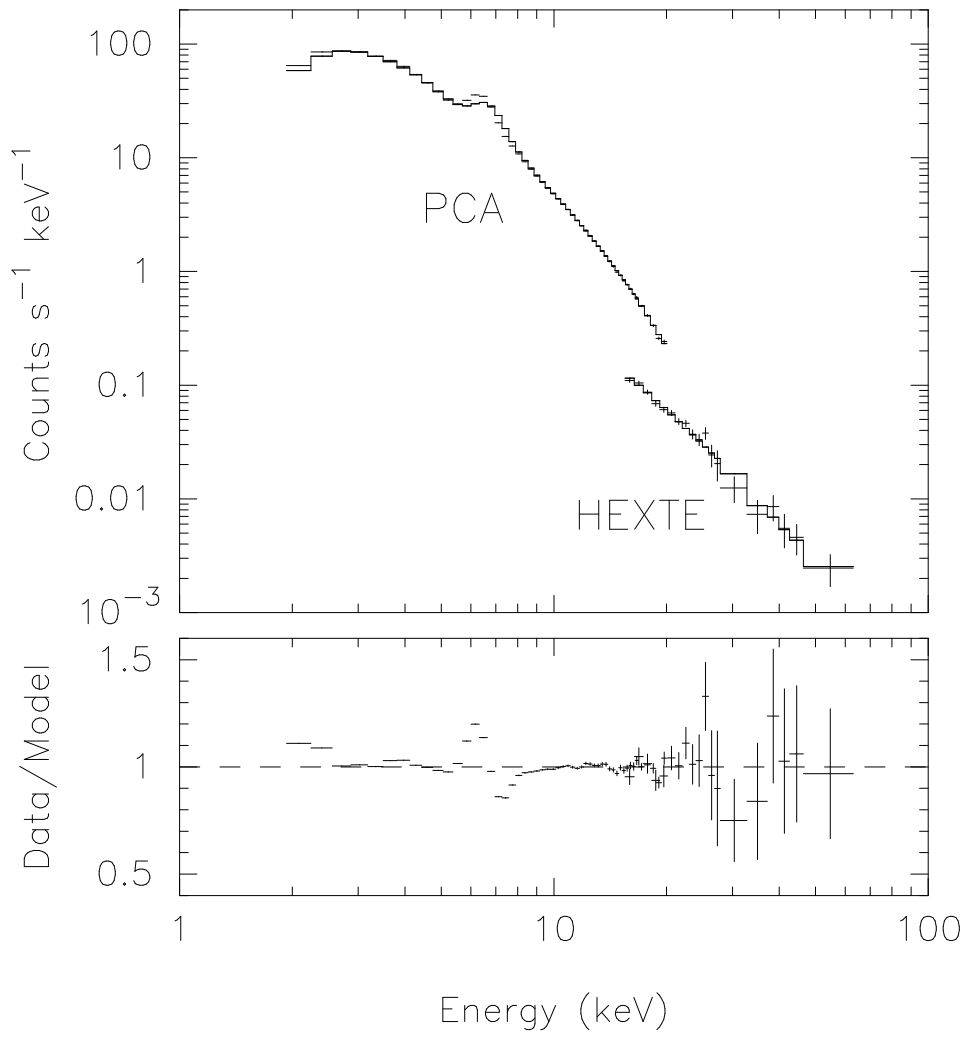


Figure 2

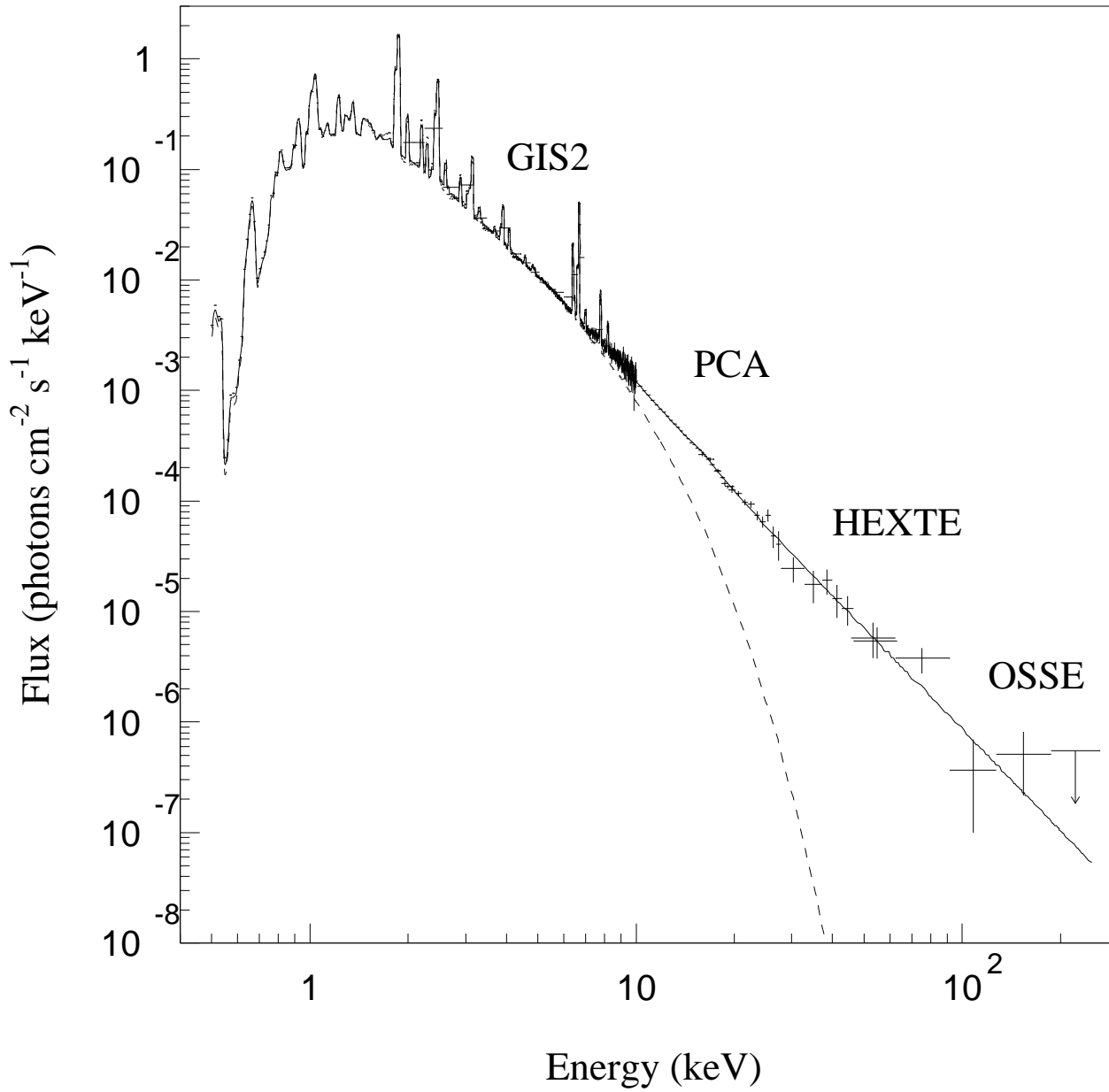


Figure 3

